Numerical Investigation of Over pressure Causes in Eugene Island P1 Sand – Part II

R. Trabelsi[1*], A. C. Seibi[2], F. Boukadi[3], W. Chalgham[4], H. Trabelsi[5]

University of Louisiana, Dept. of Petroleum Engineering, Lafayette LA, USA

Abstract— *Eugene Initial reservoir pressures from well test information were found to be higher than the calculated hydrostatic pressures. Three wells in Block 276 P1-sand had higher observed pressures than what was expected, implying pore pressures greater than anticipated. It is thought that under compaction in shaly sand and thermal dissipation from salt diapirs are the main reasons causing over pressurization. Both effects have been studied and under compaction was found to be the dominant mechanism causing pore overpressure. Transgressive shale in P1-sand, resulting from ocean transgression, acted as plastic barriers; thereby, negating the transfer of lithostatic load to deeper formations. This has resulted in constant porosities with respect to depth. A developed COMSOL multiphysics model has also indicated that temperature effects from underlying salt diapers have also affected pore pressure and that pore over pressurization by conduction was found to range from 3 – 15%.*

Keywords— Eugine Island, transgressive shale, over pressure.

I. INTRODUCTION

EI330 Normal reservoir pressure is the pressure necessary to sustain a column of water to surface (Fertl, 1976]. Normal pressures range between 0.43 and 0.50 psi/ft. Normal drilling muds weigh about 9 ppg (pounds per gallon) and exert a bottom hole pressure of approximately 0.47 psi/ft of depth. Overpressure refers to pressures higher than normal. Pressures lower than normal are called subnormal. Dickey et al. [1968] identified the location of abnormal pressures in southern Louisiana and noted that the continental and deltaic facies contain sandy beds and that the neritic (nearshore) facies also comprise a few silty and sandy beds that connect laterally to the deltaic facies. The authors added that shelf facies contains almost no sandy beds, and the pore fluids cannot escape. It was also highlighted that growth faults are seals that stop the lateral flow of pore water toward the neritic facies.

Abnormal pressure is defined as any departure from normal hydrostatic pressure at a given depth [Bruce and Bowers, 2002]. Abnormal subsurface pressures, either overpressure (geopressure) or unde rpressure, are found in hydrocarbon basins throughout the world in all lithologies, from all geologic ages, and at all depths [Fertl et al., 1994].

Timely and reliable detection of geopressure is imperative to avoid or mitigate potential drilling and safety hazards, e.g.:

- Shallow water flow
- Blowouts
- Shale instability

During drilling, advanced warning of approaching geopressuring enables mud engineers to adjust the mud weight to prevent well and reservoir damage and to determine casing points. This is a particular concern in deepwater wells where the pressure difference; i.e., the operating window, between the hydrostatic gradient and the fracture gradient is very narrow.

For most cases, shale and shaly sands are formations that exhibit over pressurization. Shale is abundant in Block 276 P1-sand with an average net to gross of 46 to 48%. A better understanding of porosity mechanics in Block 276 is of interest for many reasons, namely:

1) Shale is the dominant lithology in the block of interest basin.
2) Expulsion of pore waters from shale could affect the pressure distribution and flow of pore waters and hydrocarbons throughout the block of interest basin.
3) In many cases, shale porosity depends only on effective stress (lithostatic stress minus pore pressure), and excess shale porosity provides a useful measure of pore fluid pressure.
4) Over pressured shales pose drilling hazards and stimulate slumping and fault movement.
5) Shale porosity profiles can replicate the history of over pressuring and the time of seal formation in the area.

To interpret shale porosity, we need to know how shales compact when pore fluid pressure is hydrostatic. Hunt et al. [1998] have suggested that, in wells where fluid pressure is hydrostatic, porosity decreases linearly with depth until porosities of about 10% are reached.

At greater depths, as in the case in Block 276 P1-sand, porosity changes slightly. It goes up and down, but does not portray signs of degradation with depth. The boundary between linear (stage 1) compaction and no (stage 2) compaction occurs when the shale pores have been condensed to the thickness of about 3 mono-layers of water. For shales with a high percentage of high surface area clays (illite + smectite + illite-smectite) the limit of normal compaction can be 15-20% or even greater, according to Hunt et al. [1998). For shales with a low percentage of high surface area clays, the limit of compaction can be as low as 3%. Once shales reach stage 2 compaction, shale porosity is independent of effective stress. If pore pressure is then increased (by hydrocarbon maturation, for example), porosity will not increase and overpressures will not be revealed in shale porosity. Hunt et al. [1998] showed several examples where the top of overpressure lies in stage 2 compaction zone and porosity remains unchanged, despite the large surge in pore pressure. The perception that there is a natural limit to shale compaction provides a sound justification of these interpretations.

This contradicts with a considerable literature suggesting that porosity data can be used to predict excess (above hydrostatic) pore pressures [Magara, 1978; Fertl, 1976; Bray and Karig, 1985; Shi and Wang, 1988; Bangs et al., 1990; Luo and Vasseur, 1992, 1993; Bour et al., 1995; Gordon and Flemings, 1998; and Stump et al., 1998].

In addition, Revil et al. [1998] examined porosity-depth profiles and mud weight data in 89 wells in the Eugene Island area to determine whether the intervals of approximately constant porosity are caused by compaction reaching its natural limit or by fluid overpressure. By comparing the fluid pressures predicted from shale porosity to those computed from mud weight data, Revil et al. [1998] found that constant porosity intervals are in a state of disequilibrium compaction. The porosities were controlled by pore pressure as Gordon and Flemings [1998] reported, from an analysis of several wells in the area.

To analyze and infer the pattern of compaction, Revil et al. [1998] developed theoretical relations against which departures from hydrostatic compaction can be measured. They found that the pattern of subsurface shale porosity is spatially logical on a local scale but varies over the study area. They defined a surface where porosity commences to depart from the hydrostatic compaction trend. This surface parallels the H. sellii transgressive shale over the study area. It was proposed that the sediments become impermeable when hydrocarbon fluids entered the area and capillary seals formed [Cathles, 2001 and Shosa and Cathles, 2001], but alternative explanations are also likely.

II. RESERVOIR SIMULATION AND HISTORY MATCHING

In the attempts to history match reservoir pressure in P1-sand, pressure profiles (Fig. 1) show a significant divergence between wells #1, #12 and W-12 observed (solid) and estimated (dashed) pore pressures, during early production time. Early departures are indicative of hydrocarbon overpressure caused by under compaction and possibly heat dissipation from salt diapers in the vicinity of Block 276. The late time matching could possibly be explained by wells producing under normal hydrostatic regime after over pressured hydrocarbons have all been depleted.

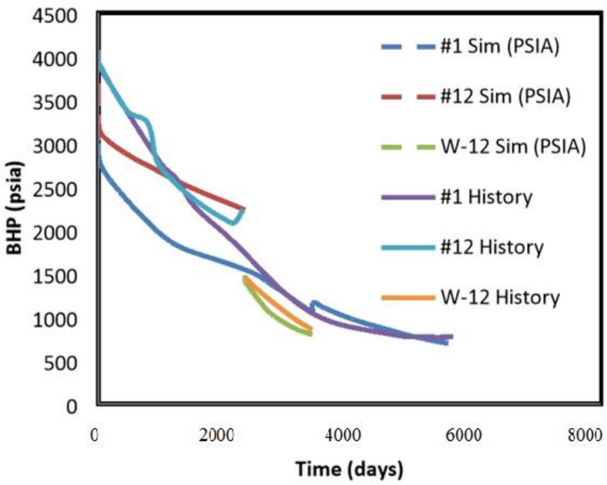

FIGURE 1: PRESSURE PROFILES IN P1 SAND, OBSERVED AND SIMULATED

In this work, it is intended to study under compaction in P1-sand, thought to be the dominant mechanism behind overpressure in Block 276. Temperature effects on pressure are also investigated.

III. ARRESTED COMPACTION

In Fig. 2 below, the depth at which porosity departs from normal compaction trend is what is referred to as fluid retention depth. At that particular depth, porosity remains constant as is the case in Block 276 P1-sand depths of 7621 to 9600 ft. It is also the depth at which pore pressure departs from the hydrostatic pressure trend and fluids become over pressured. The main attribute is what is called disequilibrium compaction.

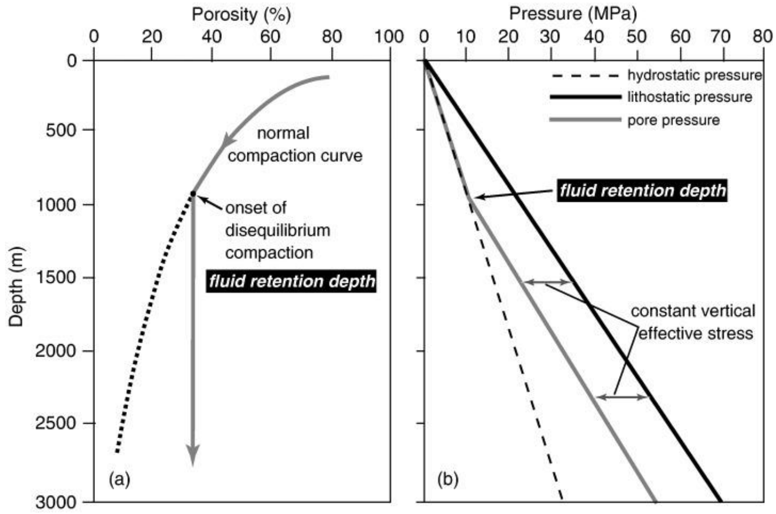

FIGURE 2: RELATIONSHIP BETWEEN (a) porosity and depth and (b) pressure and depth for a shale that becomes over pressured by disequilibrium compaction at the fluid retention depth. Modified from Harrold et al. [1999]

According to Lash and Blood [2006], the fluid retention depth in the Gulf of Mexico varies from as shallow as 0.3 mi. to as deep as 0.9 mi (Fig. 3). At that depth, shaly sandstone composition sees a drastic shift in its mineral structure. Smectite replaces most of the illite leading into water expulsion. That translates to a higher hydrocarbon storativity and higher pore pressure.

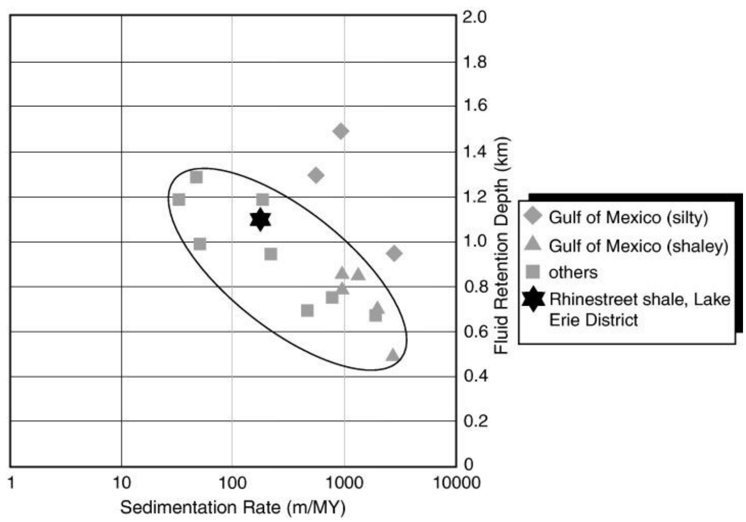

FIGURE 3: FLUID RETENTION DEPTH AS A FUNCTION OF SEDIMENTATION RATE, LASH AND BLOOD [2006]

Besides, when the sediments subside rapidly as in Fig. 3 above and in Block 276 P1-sand, fluids in the sediments can only be partially expelled. The remaining fluid in the pores must sustain all or part of the weight of overly sediments, causing the pressure of pore fluids to increase (abnormally high pore pressure). In this case, porosity decreases less rapidly than it should be with depth, and formations are said to be under-compacted or in compaction disequilibrium.

Furthermore, and according to Hunt [1996], disequilibrium compaction is caused by stepwise transformation to mixed-layer clays and illite. This releases more water into the rock and causes a slower compaction of smectite-rich rocks. Overpressures can be generated by many mechanism, such as compaction disequilibrium (under-compaction), hydrocarbon generation and gas cracking, aquathermal expansion, tectonic compression (lateral stress), mineral transformations (e.g., illitization), and osmosis, hydraulic head and hydrocarbon buoyancy [Gutierrez et al., 2006; Swarbrick and Osborne, 1998]. In nearly all cases where compaction disequilibrium has been determined to be the primary cause of over pressuring, the age of the rocks is geologically young. Examples of areas where compaction disequilibrium is cited as the primary reason of abnormal pressure include the U.S. Gulf Coast, Alaska Cook Inlet; Beaufort Sea, Mackenzie Delta, North Sea, Adriatic Sea, Niger Delta, Mahakam Delta, the Nile Delta, Malay Basin, Eastern Venezuelan Basin (Trinidad) and the Potwar Plateau of Pakistan [Law and Spencer, 1998; Burrus, 1998; Heppard et al., 1998; Powley, 1990; Nelson and Bird, 2005; Morley et al., 2011]. In these areas, the abnormally pressured rocks are mainly located in Tertiary and late Mesozoic sedimentary formations (146 to 65 mya, million years ago), the depositional setting is dominantly deltaic, and the lithology is dominantly shale, as is the case of Block 276, where sedimentary formations, Pliocene-Pleistocene (5.3 mya to 11,000) is even younger.

Additionally, Mouchet and Mitchell [1989] noted that one of major reasons of abnormal pore pressure is caused by abnormal formation compaction (compaction disequilibrium or under-compaction). When sediments compact normally, formation porosity is reduced at the same time as pore fluid is expelled. The authors added that during burial, increasing overburden pressure is the prime cause of fluid expulsion. They explained that if the sedimentation rate is slow, normal compaction occurs, i.e., equilibrium between increasing overburden and the reduction of pore fluid volume due to compaction (or ability to expel fluids) is maintained. They said that this normal compaction causes hydrostatic pore pressure in the formation. The authors explained that rapid burial, however, leads to faster expulsion of fluids in response to rapidly increasing overburden stress.

Swarbrick et al. [2002] added that the overpressures generated by under-compaction in mudrock-dominated sequences may reveal an abnormal pore pressure change with depth. They noted that the compaction disequilibrium is known by higher than expected porosities at a given depth and that the porosities deviated from the normal porosity trend.

Zhang [2011] looked at overpressure from a different angle. He plotted shale resistivity as a function of depth to explain the departure of pore pressure from the normal hydrostatic trend. The author identified under compaction as the main reason behind over pressurization. He showed that the inclined line in Fig. 4(a), above, represents the resistivity in normally compacted formation (normal resistivity, R_n). He noted that in the under-compacted section resistivity (R) reversal occurs, indicating an over pressured formation in Fig. 4(b). He showed a lower resistivity in the under compacted/over pressured section. In the figure, R_n is the normal resistivity trendline, σ_V is the lithostatic or overburden stress, σ_e is the effective vertical stress, p_n is the normal pore pressure, and p is the pore pressure.

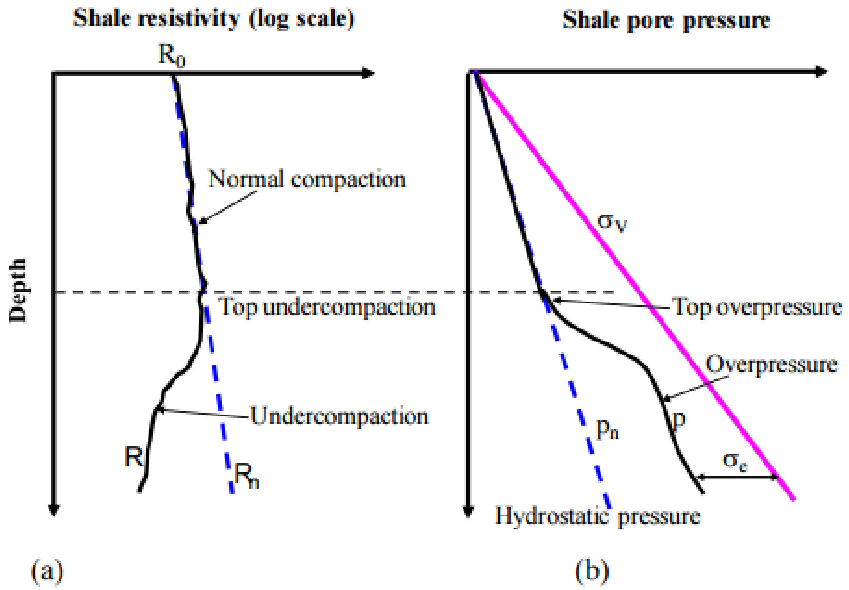

FIGURE 4: SCHEMATIC OF RESISTIVITY (A) AND PORE PRESSURE (B) IN AN UNDERCOMPACTED BASIN, ZHANG [2011]

In Fig. 5, Zhang [2011] plotted porosity as a function of depth, to prove his hypothesis. The dashed porosity profile in (a) represents normally compacted formation. In the over pressured section, the porosity reversal occurs (heavy line). In the over pressured section, porosity is larger than that in the normal compaction trendline (ϕ_n) and under compaction is apparent.

In addition, Fig. 6 below shows different tracks of porosity. Porosity of shales and normal compaction trendline. Shales do not follow the normal compaction trend.

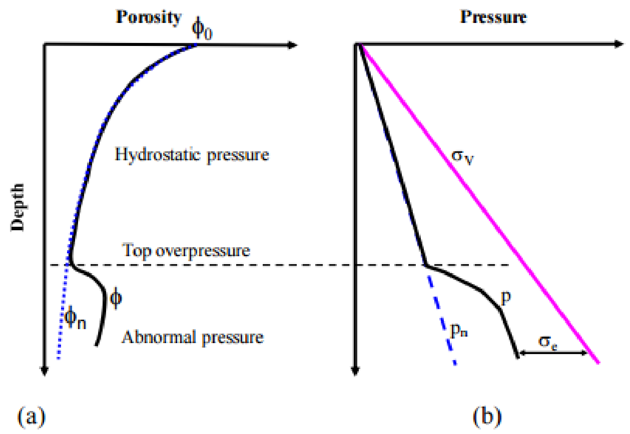

FIGURE 5: SCHEMATIC OF POROSITY (A) AND CORRESPONDING PORE PRESSURE (B) IN A SEDIMENTARY BASIN [ZHANG, 2011]

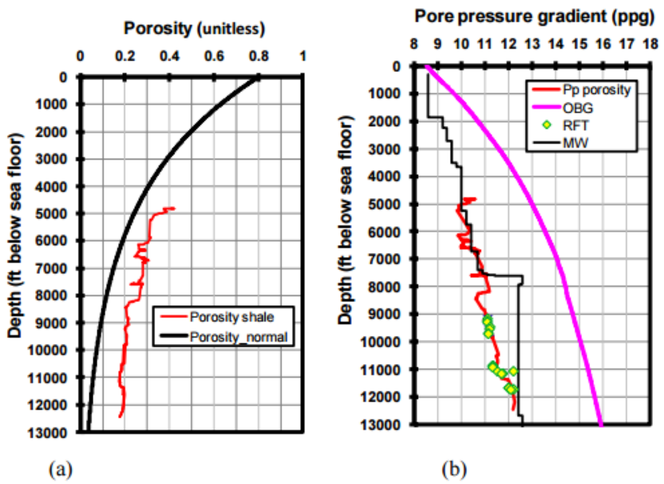

FIGURE 6: POROSITY AND PRESSURE PREDICTION FROM THE POROSITY [ZHANG, 2011]

In Fig. 7, Shaly P1-sand porosity profile shows the same behavior. No clear trend of compaction and porosity hovers around an average of 30% and stays constant with increasing depth. In Fig. 6 the normal compacted porosity should range between 12 to 10% in P1 sand.

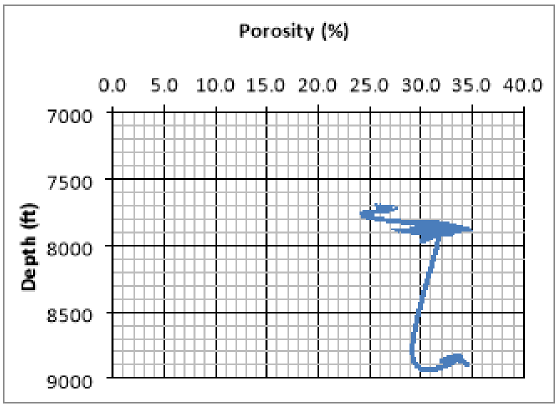

FIGURE 7: P1-SAND SIDEWALL CORE POROSITY PROFILE

Permeability profiles can also be used in justifying under compaction. Fig. 8 is an illustration of permeability variation with depth in P1-sand. A lower permeability at the top of the formation explains the occurrence of transgressive shale, a primary cause of ceased compaction. Permeability is lower in the shaly P1-sand and sees a drastic shift in the bottom of the reservoir and indicates a facies change.

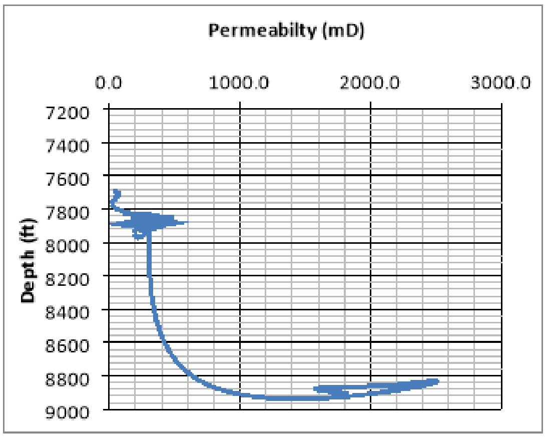

FIGURE 8: P1-SAND SIDEWALL CORE PERMEABILITY PROFILE

High water saturation distribution in layer 1 (Fig. 9) is another indication of transgressive shale in large quantities and that P1-sand is overlain by a shale barrier, as seen in Fig. 7 and 8 above.

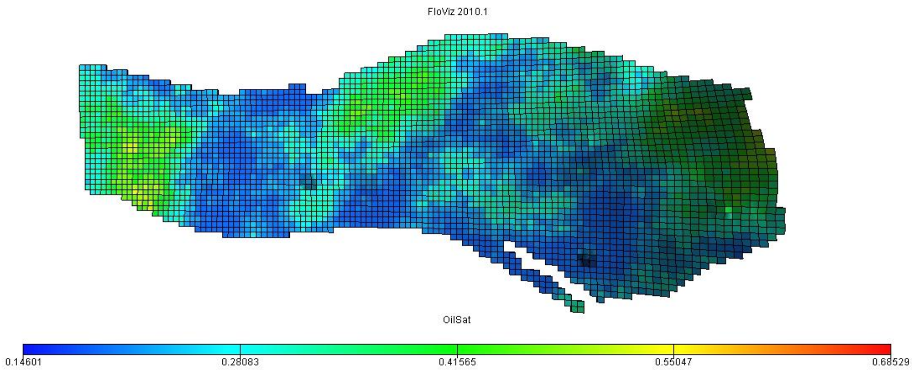

FIGURE 9: WATER SATURATION DISTRIBUTION IN LAYER 1

Techlog generated porosity and water saturation (Fig. 10) and volume of shale (Vshale) and net-to-gross (NTG) logs (Fig. 11) in wells #1, #12 and W-12 also indicate that no clear trend of compaction is evident in the shaly transgressive sand and that the porosity is under compacted (Fig. 10).

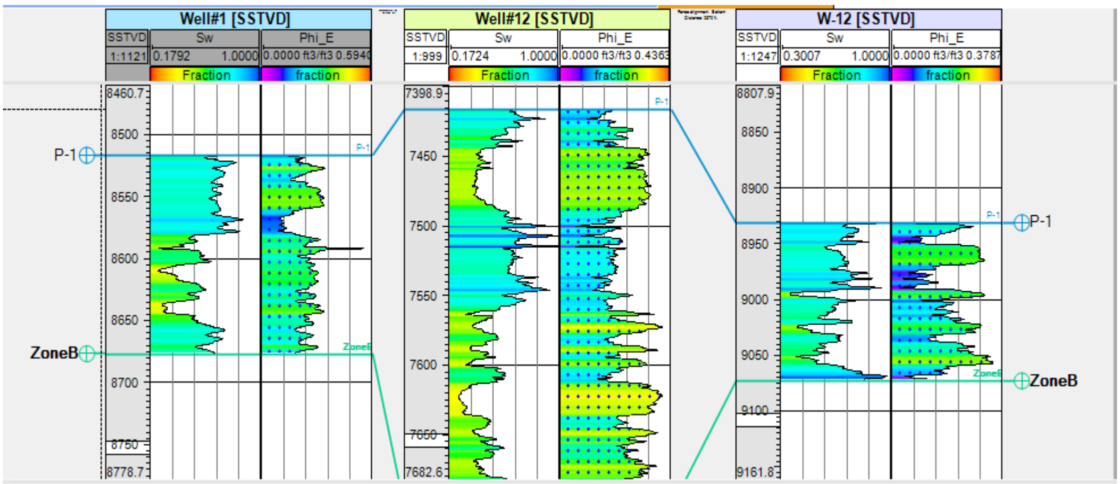

FIGURE 10: NO CLEAR TREND OF POROSITY DEGRADATION IN P1-SAND

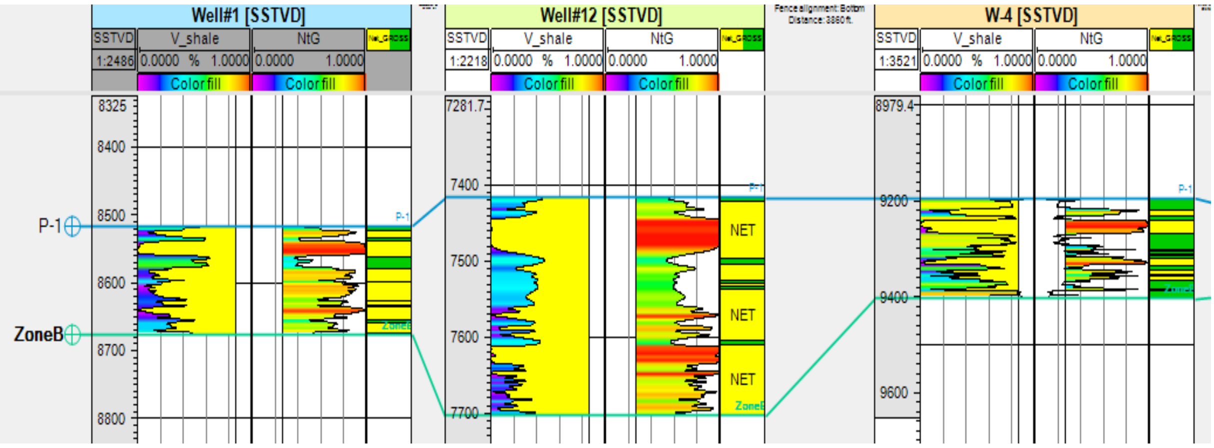

FIGURE 11: EVIDENCE OF INTERBEDDED (TRANSGRESSIVE) SHALE

To better describe porosity variation with depth and under compaction, a mathematical model is used.

IV. MATHEMATICAL MODEL

The relationship between the in-situ, porosity, $\emptyset$, and the uncompacted porosity, $\emptyset_o$, is given by [Revil *et* al., 1998]:

$$\emptyset = 1 - (1 - \emptyset_o)exp(\frac{z}{z_c}) \tag{1}$$

where, z is a depth of interest and

$$\frac{1}{z_c} = g(\rho_g - \rho_f)\emptyset_o\beta$$

where β is the compaction coefficient with β=4.8x10^{-12} psi in the Eugene Island minibasin.

In addition, we assume that fluid pressures have not increased for reasons unrelated to compaction, (2) solid material has not been dissolved and removed, (3) buoyant pressures are not transmitted horizontally or vertically.

Porosity is deduced from density logs using;

$$\rho = (1 - \emptyset)\rho_g + \emptyset\rho_f \tag{2}$$

where, ρ is the sediment density, ρ_g is the sediment grain density, and ρ_f is the pore fluid density. Generally, grain density is taken as 165.4 lb/ft^3 and pore fluid density as 62.4.

We assume that changes in porosity, $\partial\emptyset$, are explicitly related to changes in effective stress, $\partial\sigma_{eff}$:

$$\partial\emptyset = -\emptyset_o\beta\partial\sigma_{eff} \tag{3}$$

where, $\emptyset_o$ is the uncompacted porosity and β is the long term compressibility. The effective stress equals the lithostatic stress, P, minus the pore pressure p:

$$\sigma_{eff} = P - p \tag{4}$$

Lithostatic stress is related to density of mineral grains, ρ_g, density of pore fluid, ρ_f, and sediment porosity, $\emptyset$, by:

$$\partial P_z = \left(\rho_g(1 - \emptyset) + \rho_f\emptyset\right)g\Delta z \tag{5}$$

The interpretation method is straightforward. Equation (5) implies that instead of a decreasing porosity in line with normal hydrostatic compaction, a constant porosity with increasing depth implies excess fluid causing pore over pressurization. To make sure that over pressurization was mostly caused by under compaction; a stress analysis was conducted using COMSOL to study the effect of gravity and temperature on pressure and whether the shale barrier was acting as lithostatic gradient absorber, limiting compaction in P1-sand.

V. EFFECT OF TEMPERATURE ON PRESSURE VARIATION IN P1-SAND

A finite element model using COMSOL multiphysics was developed to study the effect of temperature on the effective stress (see Fig. 12). This study will also explain whether the shale barrier overlain the sand was the main reason behind under compaction. A two-dimensional model of the P1-sand was built using quadrilateral elements to determine the thermal stresses caused by heat dissipated from the salt dome and thermal boundaries. A thermal analysis was initially conducted to determine the temperature distribution within the P1-sand from which thermal stresses were obtained. To mimic the overburden stress, a pressure gradient of 1 psi/ft was assumed and an equivalent pressure of 7500 psi was applied to the top of the elemental volume. Gravity of the different sedimentary strata was also considered. The eastern and western boundaries of the reservoir were constrained from moving laterally and allowed to move vertically; whereas, the bottom side of the model was constrained from moving in all directions.

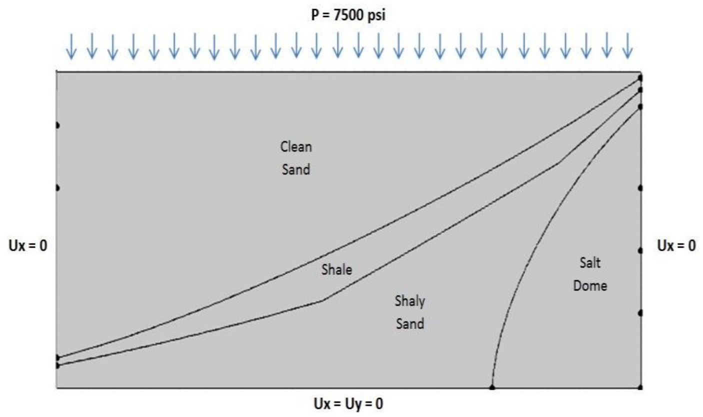

FIGURE 12: BOUNDARY CONDITIONS USED IN THE FINITE ELEMENT MODEL

Fig. 13 shows the displacement field under mechanical and thermal loads. It can be seen that the highest vertical displacement of -6.43 ft occurred at the top of the section (clean sand at a depth of 7500 ft) with least displacement below the shale layer, which acts as a visco-plastic medium; thereby, sustaining the overburben pressure causing under compaction in P1-sand. Fig. 13 also shows that shale, a visco-plastic medium, absorbs most of the stress and acts as a load carrier structure leading to under compaction in the underlain shaly sand portion of the reservoir.

To understand the effect of temperature on the pore pressure, the effective stress and pressure contours for both thermo-mechanical (gravity + temperature) and mechanical loading (gravity only) were examined. Fig.s 13(a) and (b) show the effective stress contour and pressure for gravity alone; while Figs. 13(c) and 13(d) portray the contours for gravity and temperature. A comparison between the effective stress contours reveals that temperature effect was found to contribute to the increase in pore pressure up to 20.5% increase throughout the whole field.

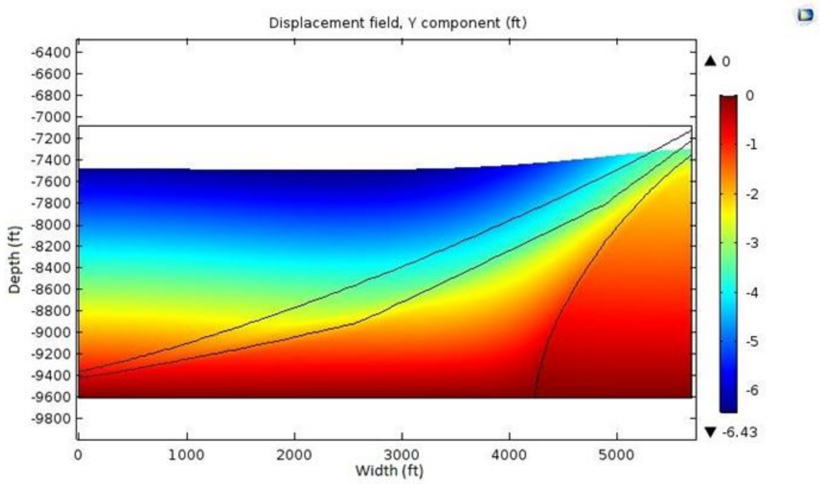

FIGURE 13: DISPLACEMENT SIMULATION CONTOUR

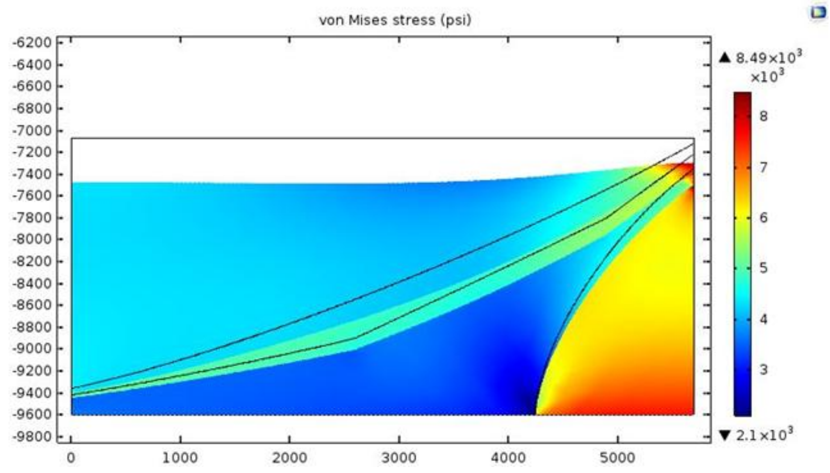

FIGURE 14(A): STRESS DISTRIBUTION IN SIMULATION CONTROL VOLUME, GRAVITY ONLY

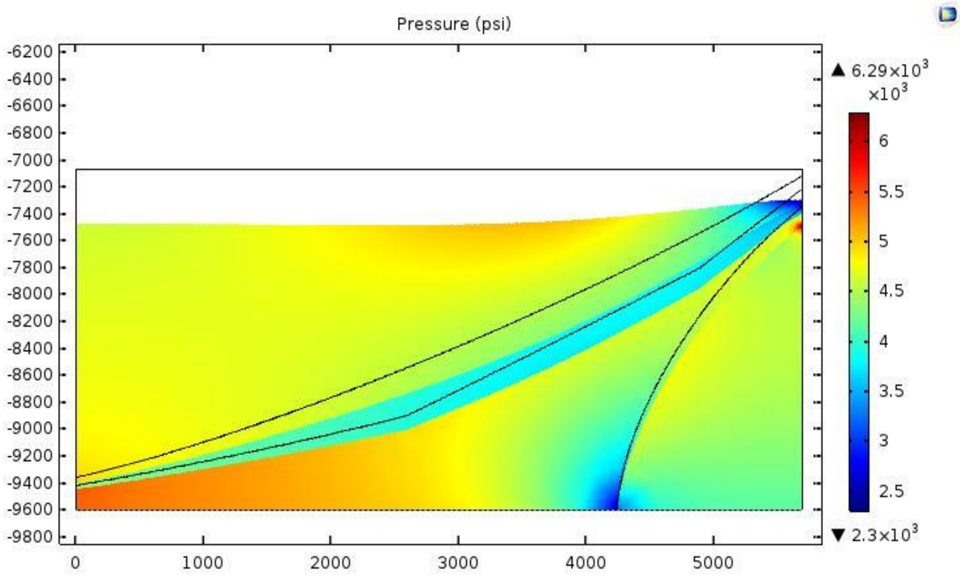

FIGURE 14(B): PRESSURE DISTRIBUTION IN SIMULATION CONTROL VOLUME, GRAVITY ONLY

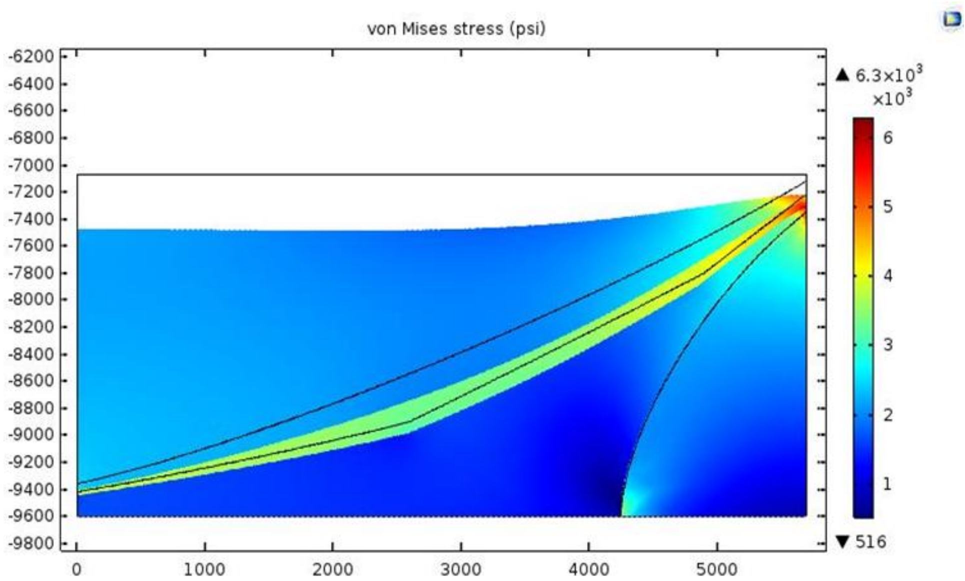

FIGURE 14(C): STRESS DISTRIBUTION IN SIMULATION CONTROL VOLUME, GRAVITY + TEMPERATURE

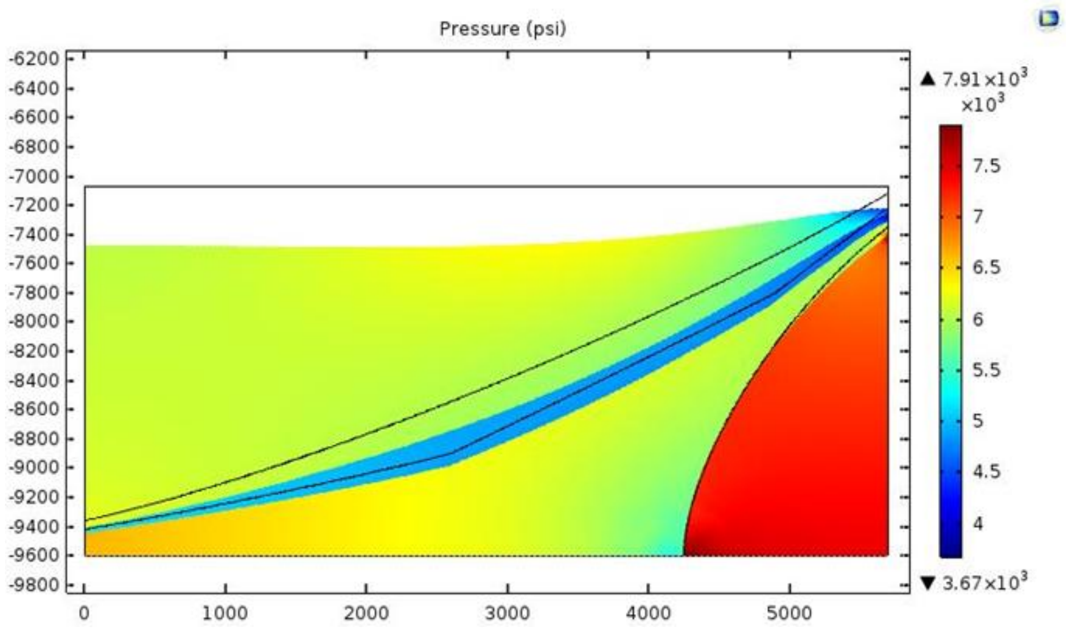

FIGURE 14(D): PRESSURE DISTRIBUTION IN SIMULATION CONTROL VOLUME, GRAVITY + TEMPERATURE

A close examination of Fig.s 13(a) and (c) exhibit that P1-sand (dark blue) is subjected to the lowest effective stress indicating that the pore pressure gets higher in this zone as compared to the clean sand layer (light blue); thereby, confirming the theory of under compaction (overpressure) presented in Equation (6).

$$\sigma_{ob} = \sigma_{eff} + p_f \tag{6}$$

Fig. 14 shows a vertical line along which pressure values were taken at different depths. It passes through well 12 in the reservoir which located below the shale layer. Fig. 15 shows the pressure profile as a function of depth for both loading cases (mechanical only versus mechanical and thermal). The plot clearly portrays that convection is insignificant (blue line lays on top of the orange). Temperature generated from the salt dome has, however, affected reservoir pressure and partially caused over pressurization. Gray and orange lines departure of 500 in clean sand, 30 in the shale barrier, and 350 in shaly sand is a clear indication that over pressurization of the P-1 sand is a combined effect of under compaction and temperature. It is worth noting that shale layer acted as a thermal barrier, indicated by the minimal temperature effect on pressure variation. Moreover, the shale layer acted as a load carrier as explained by its insignificant deformation (compaction).

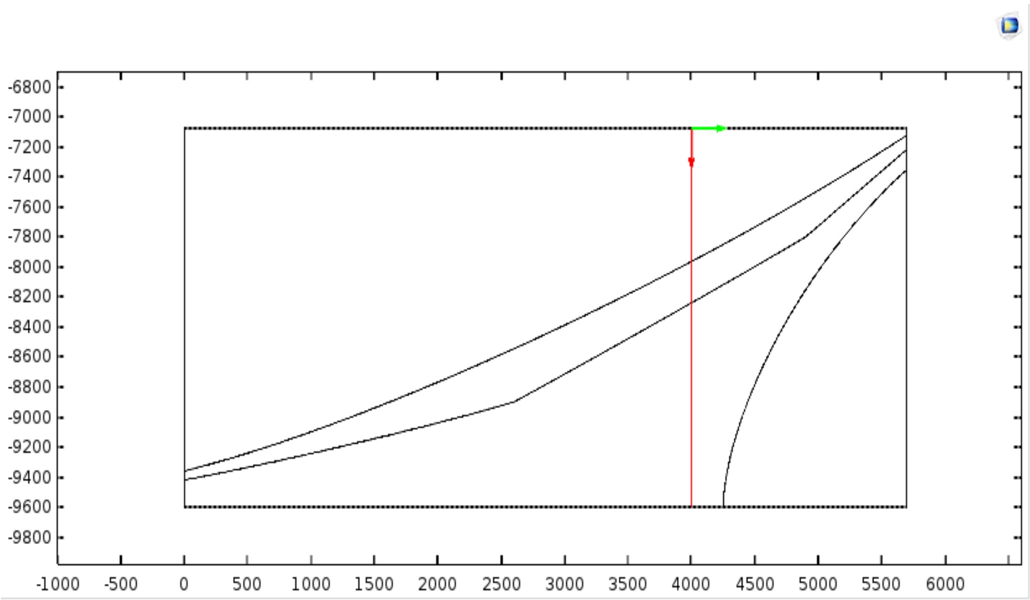

FIGURE 15: SCHEMATIC OF WELL LOCATION USED IN COMSOL SIMULATION

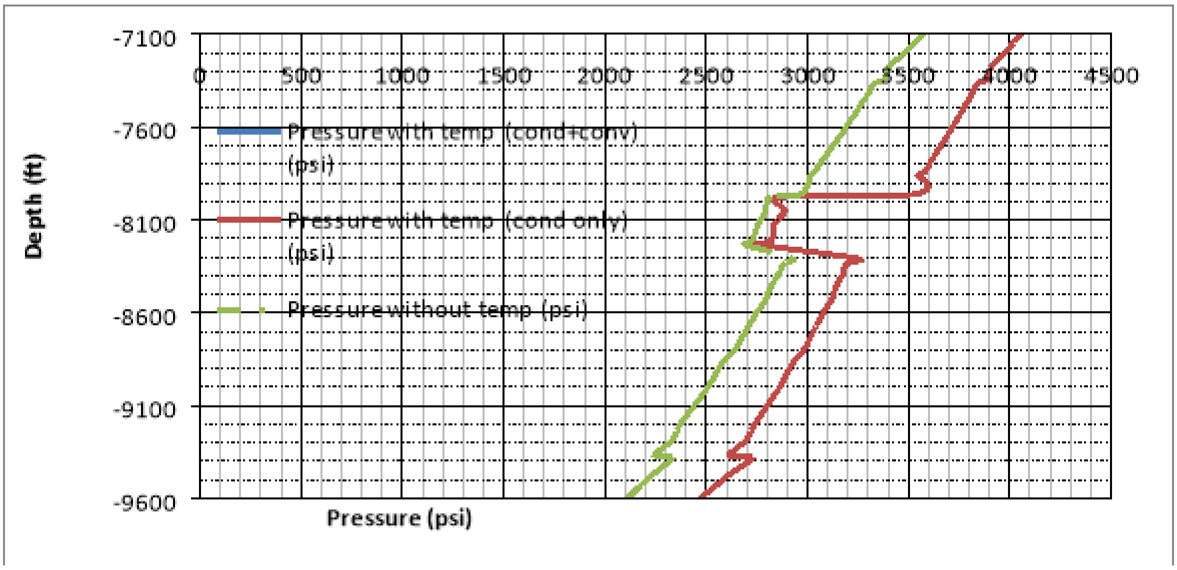

FIGURE 16: SIMULATED PRESSURE PROFILE

VI. CONCLUSIONS

Analysis of the Block 276 P1-sand porosity, permeability, shale content, and pressure show that departures of shale porosity from hydrostatic compaction trend are coherent and provide significant new information on the possible nature of under compaction. It was concluded that over pressuring is strongly controlled by depositional environment. A COMSOL Multiphysics model was also used to demonstrate that temperature effect from nearby salt diapers also contributes to over pressurization but not as much as under compaction, the dominant over pressurization mechanism. It was observed that the temperature effect on pore pressure ranges from 3 to 15%. Thereby, drilling engineers must pay attention to this increase whenever they plan for any drilling activity.

REFERENCES

[1] N. L. Bangs, G. K. Westbrook, J. W. Ladd, P. Bulh, “Seismic velocities from the Barbados Ridge complex: indicators of high pore pressures in an accretionary complex,” J. Geophys. Res., v. 95, 1990, pp. 8767-8782.

[2] O. Bour, I. Lerche, D. Grauls, “Quantitative models of very high fluid pressure: the possible role of lateral stress,” Terra Nova, v. 7, 1995, pp. 68-79.

[3] C. J. Bray, D. E. Karig, “Porosity of sediments in accretionary prisms and some implications for dewatering processes,” J. Geophys. Res., v. 90, 1985, pp. 768-778.

[4] B. Bruce, G. Bowers, “Pore Pressure Terminology,” The Leading Edge 21 (2), 2002, pp. 170–173.

[5] J. Burrus, “Overpressure models for clastic rocks, their relation to hydrocarbon expulsion: a critical reevaluation,” AAPG Memoir 70: Abnormal Pressures in Hydrocarbon Environments, 1998.

[6] G. F. Ulmishek, V. I. Slavin, “Abnormal pressures in hydrocarbon environments,” AAPG Memoir 70, 735 Chapman Petroleum geology, Elsevier1983, pp. 35–63.

[7] L. M. Cathles, “Capillary seals as a cause of pressure compartmentation in sedimentary basins,” GCSSEPM, Foundation 21st Annual Research Conference, Petroleum Systems of Deep-Water Basins Dec. 2001, pp. 561-571.

[8] P. A. Dickey, C. R. Shriram, W. R. Paine, “Abnormal pressures in deep wells of southwestern Louisiana,” Science, May 10, v. 160, 1968, pp. 609–615.

[9] B. A. Eaton, B.A., “Fracture gradient prediction and its application in oilfield operations,” Paper SPE2163. JPT, 1968, pp. 25-32.

[10] W. H. Fertl, “Abnormal formation pressure, implications for exploration, drilling, and production of oil and gas resources,” Elsevier, Amsterdam, 1976.

[11] W. H. Fertl, R. E. Chapman, R. F. Holz, “Studies in Abnormal Pressure, 1-454,” Amsterdam: Elsevier, Developments in Petroleum Science No. 38, 1994.

[12] D. S. Gordon, P. B. Flemings, “Two dimensional modeling of groundwater flow in an evolving deltaic environment,” Soc., Sedimentary Geol., v. 62, 1998, pp. 301-312.

[13] M. A. Gutierrez, N. R. Braunsdorf, B. A. Couzens, “Calibration and ranking of pore-pressure prediction models,” The leading Edge, 2006, pp. 1516-1523.

[14] T. W. D. Harrold, R. E. Swarbrick, N. R. Goulty, “Pore pressure estimation from Mudrock porosities in Tertiary Basins,” Southeast Asia. Am. Assoc. Petrol. Geol. Bull., 83, 1999, pp. 1057-1067.

[15] P. D. Heppard, H. S. Cander, E. B. Eggertson, “Abnormal pressure and the occurrence of hydrocarbons in offshore eastern Trinidad, West Indies,” Abnormal pressures in hydrocarbon environments: AAPG Memoir 70, 1998, pp. 215–246.

[16] J. M. Hunt, "Petroleum Geochemistry and Geology," W.H. Freeman, New York, 1996.

[17] J. M. Hunt, J. K. Whelan, L. B. Eglinton, L. M. Cathles III, "Relation of shale porosities, gas generation, and compaction to deep overpressures in the U.S. Gulf Coast," Abnormal pressures in hydrocarbon environments, AAPG Memoir 70, 1998, pp. 87-104.

[18] G. Lash, R. Blood, "Origin of early overpressure in the Upper Devonian Catskill Delta Complex," Western New York state, Basin Research, 19(1), 2006, pp. 51-66.

[19] B. E. Law, C. W. Spencer, "Abnormal pressures in hydrocarbon environments," Abnormal pressures in hydrocarbon environments: AAPG 777 Memoir 70, 1998, pp. 1–11.

[20] X. R. Luo, G. Vasseur, "Contributions of compaction and aquathermal pressuring to geopressure and the influence of environmental conditions," AAPG Bull., v. 76, 1992, pp. 1150-1159.

[21] X. R. Luo, G Vasseur, G., "Contributions of compaction and aquathermal pressuring to geopressure and the influence of environmental conditions," AAPG Bull., v. 77, 1993, pp. 2011-2014.

[22] K. Magara, "Compaction and Fluid Migration, Practical Petroleum Geology," Elsevier, New York, 1978.

[23] C. K. Morley, R. King, R. Hillis, M. Tingay, G. Backe, "Deepwater fold and thrust belt classification, tectonics, structure and hydrocarbon prospectivity: A review," Earth-Science Reviews, 2001, pp. 104: 41–91.

[24] J. P. Mouchet, A. Mitchell, "Abnormal Pressures While Drilling: Origins, Prediction, Detection, Evaluation," Paris: Elf EP-Editions, Editions Technip, 1989.

[25] H. N. Nelson, K. J. Bird, "Porosity-depth trends and regional uplift calculated from sonic logs, National Reserve in Alaska," Scientific Investigation Report 2005-5051, U.S. Dept. of the Interior and USGS, 2005.

[26] D. E. Powley, "Pressures and hydrogeology in petroleum basins," Earth-Sci. Rev., 29, 1990, pp. 215-226.

[27] A. Revil, L. M. Cathles, J. D. Shosa, P. A. Pezard, F. D. de Larouziers, "Capillary sealing in sedimentary basins: a clear field example, Geophys. Res. Letters, v. 25 (3), 1998, pp. 389-392.

[28] Y. Shi, C. Wang, "Generation of high pore-pressures in accretionary prism: inferences from the Barbados subduction complex," J. Geophys. Res., v. 93, 1988, pp. 8893-8910.

[29] J. D. Shosa, L. M. Cathles, "Experimental investigation of capillary blockage of two-phase flow in layered porous media," Petroleum Systems of Deep-Water Basins: Global and Gulf of Mexico Experience, GCSSEPM Proceedings Volume, 2001.

[30] B. B. Stump, P. B. Flemings, T. Finkbeiner, M. D. Zoback, "Pressure differences between overpressured sands and bounding shales at the Eugene Island 330 field (offshore Louisiana, USA) with implications for fluid flow induced by sediment loading," Overpressures in Petroleum, 1998.

[31] R. E. Swarbrick, M. J. Osborne, "Mechanisms that generate abnormal pressures: an overview," Abnormal pressures in hydrocarbon environments: AAPG Memoir 70, 1998, p. 13–34.

[32] R. E. Swarbrick, M. J. Osborne, G. S. Yardley, "Comparison of overpressure magnitude resulting from the main generating mechanisms," Pressure regimes in sedimentary basins and their prediction: AAPG Memoir 76, 2002, pp. 1–12.

[33] J. Zhang, "Pore pressure prediction from well logs: methods, modifications, and new approaches," the Science Reviews, 108(1), 2011, pp. 50-63.